PNAS

Supporting Information for

Tuft cells mediate commensal remodeling of the small intestinal antimicrobial landscape

Connie Fung, Lisa M. Fraser, Gabriel M. Barrón, Matthew B. Gologorsky, Samantha N. Atkinson, Elias R. Gerrick, Michael Hayward, Jennifer Ziegelbauer, Jessica A. Li, Katherine F. Nico, Miles D.W. Tyner, Leila B. DeSchepper, Amy Pan, Nita H. Salzman*, Michael R. Howitt*

* To whom correspondence should be addressed: M.R.H. and N.H.S.

Email: mhowitt@stanford.edu (M.R.H.), nsalzman@mcw.edu (N.H.S.)

This PDF file includes:

SI Results and Discussion

Type 2 immune induction reduces the abundance of the commensal *Enterococcus faecalis* in the small intestine. We also investigated whether type 2 immune-induced AMP alterations would decrease the abundance of other sensitive microbes, such as the Gram-positive human gut commensal *Enterococcus faecalis* (*Ef*). *Ef* is killed in vitro when incubated with purified recombinant ANG4 or SPRR2A (1, 2), AMPs that are induced with type 2 immunity. To assess the impact of type 2 immune-associated AMPs on *Ef* survival throughout the gastrointestinal (GI) tract, we first IP-injected mice with IL-25, and then orally inoculated these mice and mock-injected controls with *Ef* (SI Appendix, Fig. S8A). The small intestine, cecum, and large intestine were collected from each mouse two hours post-gavage to enumerate *Ef* colony-forming units (CFUs). We found that *Ef* CFUs were significantly lower in the small intestines of IL-25-injected mice compared to controls but not in other GI sites (SI Appendix, Fig. S8B). This shows that type 2 immune induction lowers *Ef* abundance specifically in the SI, which could reflect an inhospitable AMP environment for this bacterium. However, given that type 2 immunity is typically associated with increases in gut motility (3), we assessed GI transit in mock- and IL-25-injected mice by repeating the above experiment, but administering fluorescent microspheres by oral gavage instead of *Ef*. At two hours post-gavage, luminal contents from the same GI regions were collected to quantify the number of microspheres present. We found equivalent microspheres in the small intestines of mock- and IL-25-injected mice (SI Appendix, Fig. S8C), suggesting that IL-25 injections at this dose and time frame do not alter gut motility within this region. Altogether, these results suggest that decreased *Ef* abundance in the small intestine of type 2 immune-induced mice is likely not due to increased peristalsis but may reflect increased *Ef* killing by AMPs.

SI Materials and Methods

Resource availability. Mouse and microbial strains used in this study will be made available upon request addressed to the corresponding authors Michael R. Howitt or Nita H. Salzman.

Animal work ethics statement. All animal experiments were performed in accordance with NIH guidelines, with approval by the Institutional Animal Care and Use Committees (IACUC) of Stanford University and the Medical College of Wisconsin. Animals were housed in research animal facilities at Stanford University or the Medical College of Wisconsin that are accredited by the Association of Assessment and Accreditation of Laboratory Animal Care (AAALAC) International.

Mouse strains and husbandry. WT C57BL/6J mice (Stock #000664) were purchased from Jackson Laboratory. C57BL/6 mice *Gfi1b*$^{EGFP/+}$ mice were purchased from Jackson Laboratory (Stock #016161) and were bred in-house at Stanford University. C57BL/6 *Trpm5*$^{-/-}$ mice were generously provided by Dr. Robert Margolskee at the Monell Chemical Senses Center (4). C57BL/6 *Sucnr1*$^{-/-}$ mice were generously provided by Amgen under a materials transfer agreement. C57BL/6 *Il13*$^{-/-}$ mice were generously provided by Dr. Chi-Hao Lee at the Harvard School of Public Health (5). C57BL/6 *Pou2f3*$^{-/-}$ mice were generously provided by Dr. Craig Wilen at the Yale School of Medicine (6). *Sucnr1*$^{-/-}$ mice were bred in-house at Stanford University, and experiments were performed using co-housed WT littermates. *Pou2f3*$^{-/-}$ mice were bred in-house at Stanford University, and experiments were performed using co-housed *Pou2f3*$^{+/-}$ littermates. *Trpm5*$^{-/-}$ and *Il13*$^{-/-}$ mice were bred in-house at Stanford University and co-housed with WT controls for 2 weeks prior to use in experiments. For germ-free experiments, WT C57BL/6J mice were bred and maintained in semi-rigid isolators (Park Bioservices) under standard germ-free conditions in the Gnotobiotic Core Facility at the Medical College of Wisconsin. For 16S rRNA gene sequencing experiments, WT C57BL/6 male mice (5 weeks old; Model # B6-M MPF) were purchased from Taconic Biosciences, whose mouse colonies naturally contain segmented filamentous bacteria (SFB) as part of their microbiome (7).

Filtering and normalization of small intestinal spatial transcriptomics (ST) data. All ST data analysis was computed in R. ST spots with less than 300 genes detected or more than 50% mitochondrial gene expression were first filtered out as low-quality cells and were excluded from the analysis. The FindVariableFeatures function was used to select 2,000 variable genes with default parameters. The ScaleData function was used to scale and center the counts in the dataset. STUtility was used to process gene expression matrices for the uncolonized and *T. musculis*-colonized tissue sections using the InputFromTable function. Effectively, this merged and converted the samples into a single Seurat object.

The merged dataset was then enriched for protein coding genes by removing genes annotated with non-coding RNA. The filtered dataset was then normalized by variance stabilizing transformation using Seurat's SCTransform.

Visualization of spatial expression. STUtility (8) offers a variety of native tools to visualize the expression of genes on the tissue. We took advantage of the FeatureOverlay function to visualize our genes of interest. Moreover, the VlnPlot function in Seurat was used to visualize relative changes in gene expression between the samples.

Deconvolution of ST data. Using non-negative matrix factorization (NNMF), the spatially-resolved transcriptomic data set was split into the respective uncolonized and *T. musculis*-colonized samples and deconvolved into 20 factors. A second mode of analysis included integrating the two sample datasets and deconvolving 20 factors resulting in gene modules and cell topics that described the data. Using the NNMF modes as the reduction, Harmony was used to integrate the uncolonized and *T. musculis*-colonized sample using the SCT assay values. 8 clusters were created and further defined by the top 5 genes with the largest log-2 fold change. Differential expression analysis (DEA) was conducted using FindAllMarkers from Seurat to detect marker genes for each cluster.

Moreover, we leveraged an existing small intestinal epithelial single-cell RNA sequencing (scRNA-seq) dataset (9) to map onto our ST dataset using the FindTransferAnchors within Seurat. This function constructs a weight matrix that defines the association between each query cell in the reference dataset and each anchor in the spatial dataset. These weights sum to 1 and were used as the percentage of the cell type in the spots. This results in a predicted ID score for the probability of the annotated cells present within the ST dataset. We used these predicted ID scores to discern the presence of certain epithelial cells on our tissue in an unbiased way.

R packages used for ST data analysis. The R packages used to analyze and plot the ST data as described include: BiocManager v1.30.16; Cowplot v1.1.1; datasets v4.1.2; dittoseq v1.6.0; ggplot2 v3.3.5; graphics v4.1.2; grDevices v4.1.2; harmony v0.1.0; magrittr v2.0.3; methods v4.1.2; NMF v0.24.0; NNLM v0.4.4; pheatmap v1.0.12; progeny v1.16.0; Seurat v4.1.0; SeuratObject v4.0.4; stats v4.1.2; STUtility v0.1.0; swne v0.6.20; tidyverse v1.3.1; utils v4.1.2; zeallot v0.1.0.

***Tritrichomonas musculis* enumeration.** *T. musculis* (*T. mu*) numbers in the distal small intestine were enumerated as previously described (10, 11). Briefly, the distal 10 cm of the small intestine (ileum) was removed and flushed with ice-cold sterile phosphate-buffered saline (PBS) using a 19-gauge feeding needle. The intestinal contents were pelleted by centrifugation at 2000x*g* for 5 minutes and stored at -20ºC. Genomic DNA was isolated from the intestinal contents with the DNeasy PowerSoil Kit (Qiagen) according to the manufacturer's instructions. To detect and enumerate *T. mu*, qPCR was performed using the PowerUp SYBR Green Master Mix (Applied Biosystems) with the following primers recognizing *the T. musculis* 28S rRNA gene: *T. musculis* 28S rRNA for and *T. musculis* 28S rRNA rev (see Table S1 for primer sequences). To convert qPCR Ct values into protist numbers, we used a previously published standard curve that was generated using known amounts of *T. mu* (10).

Epithelial cell isolation and flow cytometry. For most experiments in this study, the distal 10 cm of the small intestine (ileum) was removed and flushed with ice-cold sterile PBS using a 19-gauge feeding needle. For experiments that involved the proximal small intestinal regions, the proximal 7 cm of the small intestine was removed for the duodenum, and the next 10 cm following that was removed for the jejunum and similarly flushed. The tissues were then opened longitudinally, Peyer's patches were removed, and the remaining tissue was gently agitated at 4ºC in PBS, 2% heat-inactivated FBS (iFBS), 5 mM HEPES, and 1 mM DTT for 10 minutes. Then, the tissue was transferred into pre-warmed PBS with 2% iFBS, 5 mM HEPES, and 5 mM EDTA and shaken at 37ºC for 15 minutes, followed by vigorous shaking to strip off the epithelial cells. This was repeated once more, and epithelial cells from both fractions were combined and washed with PBS. Afterwards, the epithelium was digested in DMEM containing 10% iFBS, 0.5 U/mL Dispase II (StemCell Technologies), and 50 µg/mL DNase (Alfa Aesar) for 10 minutes at 37ºC. The resulting solution was passed through 70 µm filters and washed in PBS containing 2% iFBS and 1 mM EDTA. The resulting single-cell suspension was blocked with anti-CD16/CD32 (Clone 93, BioLegend), and then stained with the following antibodies: PacBlue-conjugated anti-CD45 (Clone 30-F11, BioLegend),

Phycoerythrin/Cyanine7 (PE/Cy7)-conjugated anti-EpCAM (Clone G8.8, BioLegend), and AlexaFluor 647-conjugated anti-Siglec-F (Clone E50-2440, BD Biosciences). Cell viability was assessed by propidium iodide (BioLegend) staining. Cells were analyzed on a BD FACS Canto II. Epithelial cells were gated on viable $CD45^-EpCAM^+$ cells. Tuft cells were further selected as $SiglecF^+$ (gating strategy shown in Fig. S11). For experiments that involved *Gfi1b*$^{EGFP/+}$ mice, in which tuft cells are specifically marked with EGFP, the single-cell suspension was stained with the following antibodies: PacBlue-conjugated anti-CD45 (Clone 30-F11, BioLegend) and APC-conjugated anti-EpCAM (Clone G8.8, BioLegend). Epithelial cells were gated on viable $CD45^-EpCAM^+$ cells. Tuft cells were further selected as $EGFP^+$. Information on flow reagents is listed in Table S2.

Transmission electron microscopy. The distal small intestines from uncolonized or *T. musculis*-colonized mice were harvested. A 1 cm long piece of the most distal part of the intestinal tube was cut and immersed in Karnovsky's fixative—2% glutaraldehyde and 4% paraformaldehyde in a 0.1M sodium cacodylate buffer, pH 7.4, at room temperature (RT). After the intestinal tubes had been immersed for about 15 minutes, a scalpel was used to cut 1-3 mm rings from the intestinal tubes. These intestinal rings were fixed for an additional hour at RT, and then submitted to the Cell Sciences Imaging Facility at Stanford University for further sample processing. The fix was replaced with cold-aqueous 1% osmium tetroxide and then allowed to warm to RT for 2 hours rotating in a hood, washed 3X with ultrafiltered water, then en bloc stained in 1% uranyl acetate at RT for 2 hours while rotating. Samples were then dehydrated in a series of ethanol washes for 30 minutes each at RT beginning at 50%, then 70% ethanol, and then moved to 4ºC overnight. Afterwards, the samples were placed in cold 95% ethanol and allowed to warm to RT, changed to 100% ethanol 2X, and then propylene oxide (PO) for 15 minutes. Samples were infiltrated with Embed-812 mixed 1:2, 1:1, and 2:1 with PO for 2 hours each, with samples left in 2:1 resin to PO overnight, rotating at RT in a hood. The samples are then placed into Embed-812 for 2 to 4 hours, placed into molds with labels and fresh resin, oriented, and placed into a 65ºC oven overnight. Sections were taken around 80 nm using an UC7 (Leica, Wetzlar, Germany), picked up on formvar/Carbon-coated 100 mesh Cu grids, stained for 40 seconds in 3.5% uranyl acetate in 50% acetone, followed by staining in Sato's Lead Citrate for 2 minutes. Samples were observed in the JEOL JEM-1400 120kV electron microscope. Images were taken using a Gatan Orius 832 rk X 2.6k digital camera with 9 µm pixels.

Histology and fluorescence microscopy. The distal small intestine was removed and fixed in 4% PFA diluted in PBS at 4˚C overnight, zinc formalin at room temperature overnight, or Carnoy's solution at room temperature overnight. The tissue was then embedded in paraffin and cut into 4 µm-thick sections. H&E or Alcian blue staining was performed using standard procedures by the Stanford Pathology Department Histology Service Center or the Core Histology Facility at the Children's Research Institute (CRI), Children's Wisconsin. For immunofluorescence, heat-mediated antigen retrieval was performed in sodium citrate buffer (10 mM sodium citrate, 0.05% Tween 20, pH 6.0) for 20 minutes. Then, the slides were washed in PBS and blocked in PBS containing 3% BSA, 2% goat serum, and 0.1% saponin for 1 hour at room temperature. Primary antibodies were incubated at 4ºC overnight, and secondary antibodies were incubated for 1 hour at room temperature. Primary antibodies used include: Rabbit anti-DCLK1 (1:200 dilution, Abcam), Mouse anti-E-Cadherin (1:400 dilution, BD Biosciences), Rabbit anti-Lysozyme (1:500 dilution, Agilent), Rabbit anti-RELMβ (1:200 dilution, PeproTech), Rabbit anti-MUC2 (1:200 dilution, Abcam), and DNA was labeled with DAPI (0.5 µg/mL). Samples were washed and then mounted in VECTASHIELD Antifade Mounting Medium (Vector Laboratories). Images were captured with a Zeiss LSM 700 confocal microscope (Carl Zeiss, Oberkochen, Germany) or a Nikon Eclipse E400 microscope (Nikon). Information on antibodies used is listed in Table S2.

Paneth cell enumeration and size measurements. Paneth cells were identified using H&E-stained slides. For Paneth cell counts, only crypts that were aligned along the longitudinal axis such that the crypt lumen could be seen were evaluated. Granule-containing Paneth cells per crypt were manually counted on a Nikon Eclipse E400 microscope (Nikon) or from scanned slide images. Slides were scanned and digitized by the Imaging Core at the Children's Research Institute, Children's Wisconsin using a Hamamatsu slide scanner or by the Stanford Pathology Department Histology Service Center using an Aperio AT2 slide scanner (Leica). Image analysis of scanned slides was conducted manually using OlyVIA (Olympus). Paneth cell enumeration was represented as the average number of Paneth cells per crypt.

To measure Paneth cell size, granule-containing Paneth cells were annotated using the closed polygon annotation tool in QuPath to outline individual cells. After Paneth cells in 10 crypts per sample were annotated, the area for each Paneth cell was determined using the annotation results function in QuPath. Then, the average Paneth cell area was determined by summing up the areas of all measured Paneth cells and dividing by the total number of annotated Paneth cells per sample. A minimum of 24 Paneth cells were annotated per sample, and only Paneth cells from crypts that were aligned along the longitudinal axis such that the crypt lumen could be seen were included in the analysis. Paneth cell area was represented as the average μm^2.

Tuft cell enumeration via immunofluorescence microscopy. Tuft cells were identified by immunofluorescence microscopy using DCLK1 staining as described above. Images were acquired using a VS120 slide scanner (Olympus) at the Imaging Core at the Children's Research Institute, Children's Wisconsin. Image analysis was conducted manually using QuPath. First, the polyline tool was used to measure 20 crypt-villus axis lengths per ileum, using the DAPI and E-Cadherin channels as reference. Next, the DCLK1 channel was used as reference to enumerate tuft cells among the previously established regions of interest. Tuft cell enumeration was represented as the number of tuft cells per mm crypt-villus axis.

RNA isolation and quantitative reverse transcription PCR (qRT-PCR) for in vivo and in vitro samples. For RNA isolation from total epithelium from the distal small intestine (samples from Fig. 3, 5, and 7), the epithelial fraction was collected and lysed in Qiazol (Qiagen) for RNA extraction according to the manufacturer's instructions. For small intestinal organoids, whole organoids were lysed in Qiazol, and RNA was extracted accordingly. RNA concentrations were determined using a NanoDrop. RNA was DNase-treated using the TURBO DNA-free Kit (ThermoFisher Scientific), and then cDNA was synthesized using the iScript cDNA Synthesis Kit (Bio-Rad). qRT-PCR was performed using the PowerUp SYBR Green Master Mix (Applied Biosystems).

For samples from Fig. 4, freshly collected or RNAlater (ThermoFisher Scientific)-preserved sections of the distal small intestine were manually homogenized using a pestle tissue grinder assembly and RNA was extracted using a RNeasy minikit (Qiagen) following the manufacturer's instructions. RNA was DNase-treated using the TURBO DNA-free kit (ThermoFisher Scientific). RNA was further purified using sodium acetate precipitation. RNA concentrations were determined using a NanoDrop, and cDNA synthesis was performed using the iScript cDNA Synthesis Kit (Bio-Rad). qRT-PCR was performed using the iTaq Universal SYBR Green Supermix (Bio-Rad).

For all qRT-PCR experiments, relative expression was normalized to *Gapdh*. All qRT-PCR primer sequences are listed in Table S1.

Immunoblotting. The distal small intestine was removed and flushed with ice-cold sterile PBS using a 19-gauge feeding needle. The ilea were opened longitudinally and then snap-frozen in liquid nitrogen. When ready for processing, the ilea were thawed and homogenized in 2 mL of RIPA buffer and 20 µL HALT protease inhibitor cocktail (100x) using a handheld electronic tissue homogenizer. The homogenates were then incubated on a shaker at 4ºC for 20 minutes to extract intracellular proteins. The homogenates were pelleted by centrifugation at 16000*xg* for 15 minutes at 4ºC. The supernatants, which contain extracted proteins, were transferred to new tubes and pelleted once again at the same settings to remove any residual debris. Protein concentrations for each sample were determined using the Pierce BCA Assay Kit. Equivalent amounts of extracted intracellular proteins (10-20 µg) were separated by SDS-PAGE and transferred onto PVDF membrane. The PVDF membrane was blocked in LI-COR Intercept blocking buffer (LI-COR Biosciences) for one hour, and lysozyme was detected using a Rabbit anti-Lysozyme antibody (1:10000 dilution, Abcam), followed by an IRDye® 800CW Goat anti-rabbit IgG (H+L) or IRDye® 800CW Donkey anti-rabbit IgG (H+L) secondary antibody (LI-COR Biosciences). The blot was then scanned and imaged on a LI-COR Odyssey Imager. REVERT total protein stain (LI-COR Biosciences) was used for normalization of lysozyme levels. Information on antibodies used is listed in Table S2.

In vivo IL-25 injections. Mice were intraperitoneally (IP)-injected every other day with 500 ng of recombinant IL-25 (R&D Systems; Cat# 7909-IL-010/CF) or equivalent volume of sterile PBS (vehicle control) over the course of one week. The distal small intestine was harvested to examine the abundance of tuft cells, expression of tuft cell markers and AMP-encoding genes, and Paneth cell morphology and numbers as described above.

Small intestinal organoid culture. Distal small intestinal organoids were prepared as previously described (10, 12, 13). When indicated, IL-13 (10 ng/mL) (BioLegend; Cat# 575902), IL-5 (10 ng/mL) (BioLegend; Cat# 581502), or IL-9 (10 ng/mL) (BioLegend; Cat# 556002) were added to L-WRN growth media for 2 days.

Small intestinal organoid imaging. Small intestinal organoids embedded in Matrigel were seeded onto circular glass coverslips, allowed to grow, and then treated with the desired conditions. Afterwards, the samples were fixed in 2% PFA at 4°C overnight. The samples were washed in PBS 3x the next morning and stored in PBS at 4°C until further processing. For immunofluorescence, organoids were incubated with primary antibodies diluted into PBS containing 3% BSA and 0.2% Triton X-100 overnight at room temperature. Next morning, the samples were washed in PBS 3x, and secondary antibodies were incubated for 3 hours at room temperature. Samples were washed in PBS 3x and then mounted in VECTASHIELD Antifade Mounting Medium (Vector Laboratories). Primary antibodies used include: Rabbit anti-Lysozyme (1:100 dilution, Agilent) and Rabbit anti-RELMβ (1:100 dilution, PeproTech). DNA was labeled with DAPI (0.5 µg/mL) and F-actin was labeled with AlexaFluor™ 660 Phalloidin (ThermoFisher Scientific). Images were captured with a Zeiss LSM 700 confocal microscope (Carl Zeiss, Oberkochen, Germany). Information on antibodies used is listed in Table S2.

Total bacteria and segmented filamentous bacteria (SFB) 16S rRNA gene copy number enumeration. To quantify the number of total bacterial or SFB 16S rRNA gene copies in the ileal mucosal and luminal fractions, qPCR was performed with primers recognizing total bacteria (UniF340 and UniR514) or SFB (SFB736F and SFB844R) (see Table S1 for primer sequences). Absolute quantification of 16S rRNA gene copies was determined using standard curves that were constructed using previously published plasmids that contain 16S rRNA genes specific to each group analyzed (total bacteria or SFB) (14). To track SFB 16S rRNA gene copy number prior to IL-25 injections, we collected fecal pellets from the animals at the specified timepoints, isolated genomic DNA from the feces, and used the same procedure as described above to detect and enumerate SFB 16S rRNA gene copies.

Sample processing and DNA extractions for 16S rRNA gene sequencing. WT Taconic mice were IP-injected with PBS or IL-25 as described above. At the experimental endpoint, the distal 10 cm of the small intestine was harvested from both mouse groups. The terminal 1 cm was removed for histological analysis, and the remaining 9 cm were separated into mucosal and luminal fractions. For isolation of luminal contents, the ileum was flushed with ice-cold sterile PBS using a 19-gauge feeding needle, and then pelleted by centrifugation at 2000x*g* for 5 minutes. The supernatants were removed, and the luminal contents were saved for further processing. The remaining ileal tissue was used for the mucosal fraction. Genomic DNA was extracted from the mucosal and luminal fractions using the DNeasy PowerSoil Kit (Qiagen). DNA was sent to UW-Madison Biotechnology Center for 16S rRNA gene sequencing. The V3/V4 region (341-806) of the 16S rRNA gene was amplified by PCR (341F_primer: CCTACGGGNGGCWGCAG, 806R_primer: GACTACHVGGGTATCTAATCC) and sequenced on the MiSeq platform (Illumina) using 2 x 300 base pair paired-end protocol, which yielded paired-end reads.

16S rRNA gene sequencing data analysis. QIIME2 (v. 2022.2) was used to analyze the paired-end 16S rRNA gene sequencing reads (15). Sequences were imported and summarized to check quality. Cutadapt was used to trim primers from the reads (16). Representative sequences were chosen using DADA2, which also removes chimeric sequences (17). The representative sequences were then aligned (18), masked for hypervariable regions (19), and phylogenetic trees were produced (20). A *classifier* was generated to assign taxonomy to the reads using the 99% similarity files of the SILVA v. 138 and the 341-806 region (V3/V4) of the 16S rRNA gene (21). Taxonomy was assigned to the feature table to make taxonomy bar plots and to generate relative abundance tables. Diversity metrics were run using the *core-metrics-phylogenetic* command of QIIME2. Alpha and beta diversity were analyzed using their respective commands, *alpha/beta-group-significance* (22–24). Alpha diversity metrics used a Kruskal-Wallis test to test for significance, while beta diversity metrics used a PERMANOVA test to test for significance; both types of metrics used Benjamini-Hochberg multiple comparison tests. Principal Coordinate Analysis (PCoA) plots were examined using EMPeror (25, 26) and finalized figures were made using Python (27). LEfSe, Linear discriminant analysis (LDA) Effect Size, was run to determine enriched organisms for each treatment group (28). Final

LEfSe figures were generated using Inkscape v. 1.0.1 (https://inkscape.org/). Cladograms were generated using GraPhlAn (29).

SFB in vivo killing experiments. C57BL/6 *Il13*$^{-/-}$ mice were co-housed with C57BL/6 WT mice purchased from Taconic Biosciences for two weeks to acquire SFB prior to PBS or IL-25 injections. IP injections were then conducted as described above. The distal small intestine was removed and flushed with ice-cold sterile PBS using a 19-gauge feeding needle to remove the intestinal contents. Then, a pipette tip was used to gently scrape the mucosal surface to collect mucus and mucosa-associated bacteria (mucosal fraction). Genomic DNA was extracted from the mucosal fractions using the DNeasy PowerSoil Kit (Qiagen), and the number of SFB 16S rRNA gene copies was quantified by qPCR as described above.

***Enterococcus faecalis* culture.** *E. faecalis* strain OG1RF (30) was cultured aerobically at 37ºC in Mueller-Hinton (MH) broth (BD Life Sciences) supplemented with 50 µg/mL rifampin (Rif) (Chem-Impex Int'l Inc.), or on MH agar plates supplemented with 200 µg/mL Rif.

In vivo bacterial abundance assays with *E. faecalis*. Mice were injected with either PBS (vehicle control) or 500 ng IL-25 every other day for seven days. On the day of the assay, mice were fasted for two hours and then given a single dose of $1x10^9$ *E. faecalis* strain OG1RF via oral gavage. Mice were euthanized and intestinal organs (small intestine, cecum, and large intestine) containing luminal contents were collected two hours post-gavage. Intestinal organs were individually homogenized in 2 mL of ice-cold PBS, serially diluted in autoclaved MilliQ water, and cultured on MH-Rif agar overnight at 37ºC to enumerate *E. faecalis* CFUs in each organ.

Gut motility assays. Mice were injected with either PBS (vehicle control) or 500 ng IL-25 every other day for seven days. On the day of the assay, mice were fasted for two hours and then given a single dose of $1x10^6$ 10 µm Fluoresbrite® YG carboxylate microspheres (Polysciences) via oral gavage. At two hours post-gavage, mice were euthanized and luminal contents from the small intestine, cecum, and large intestine were collected. Microspheres were manually counted using a Nikon Eclipse E400 microscope and reported as total microspheres per organ.

Statistical analysis. Statistical analysis of the spatial transcriptomics data and 16S rRNA gene sequencing data are reported in the corresponding Materials and Methods sections. Statistical tests used to compare differences between treatment groups in individual experiments are indicated in the figure legends. Student's *t*-tests were used to determine statistical significance when a parametric test was appropriate; Mann-Whitney *U* tests were used when a non-parametric test was appropriate. Ordinary one-way ANOVA tests (and corresponding multiple comparison tests) were used to determine statistical significance in experiments that require comparisons of multiple experimental groups. A generalized linear model (GLM) with negative binomial distribution was performed to compare microbial count data. A linear mixed model (LMM) was used to determine statistical significance for quantitative western blot data. SAS 9.4 (SAS Institute Inc., Cary, NC) and GraphPad Prism were used to perform all statistical analyses. $p < 0.05$ was considered statistically significant. NS indicates no statistical significance, * $p < 0.05$, ** $p < 0.01$, *** $p < 0.001$, and **** $p < 0.0001$. GraphPad Prism software was used to generate all figures, unless otherwise indicated. Center values are arithmetic means, and error bars are standard error of the mean (SEM) in figures where Student's *t*-tests, and ANOVA and LMM with multiple comparison adjustments were used to determine statistical significance. Center values are medians, and error bars are the interquartile range (IQR) in figures where Mann-Whitney *U* tests were used to determine statistical significance. For log-transformed data, center values are geometric means, and error bars are the 95% confidence interval (CI).

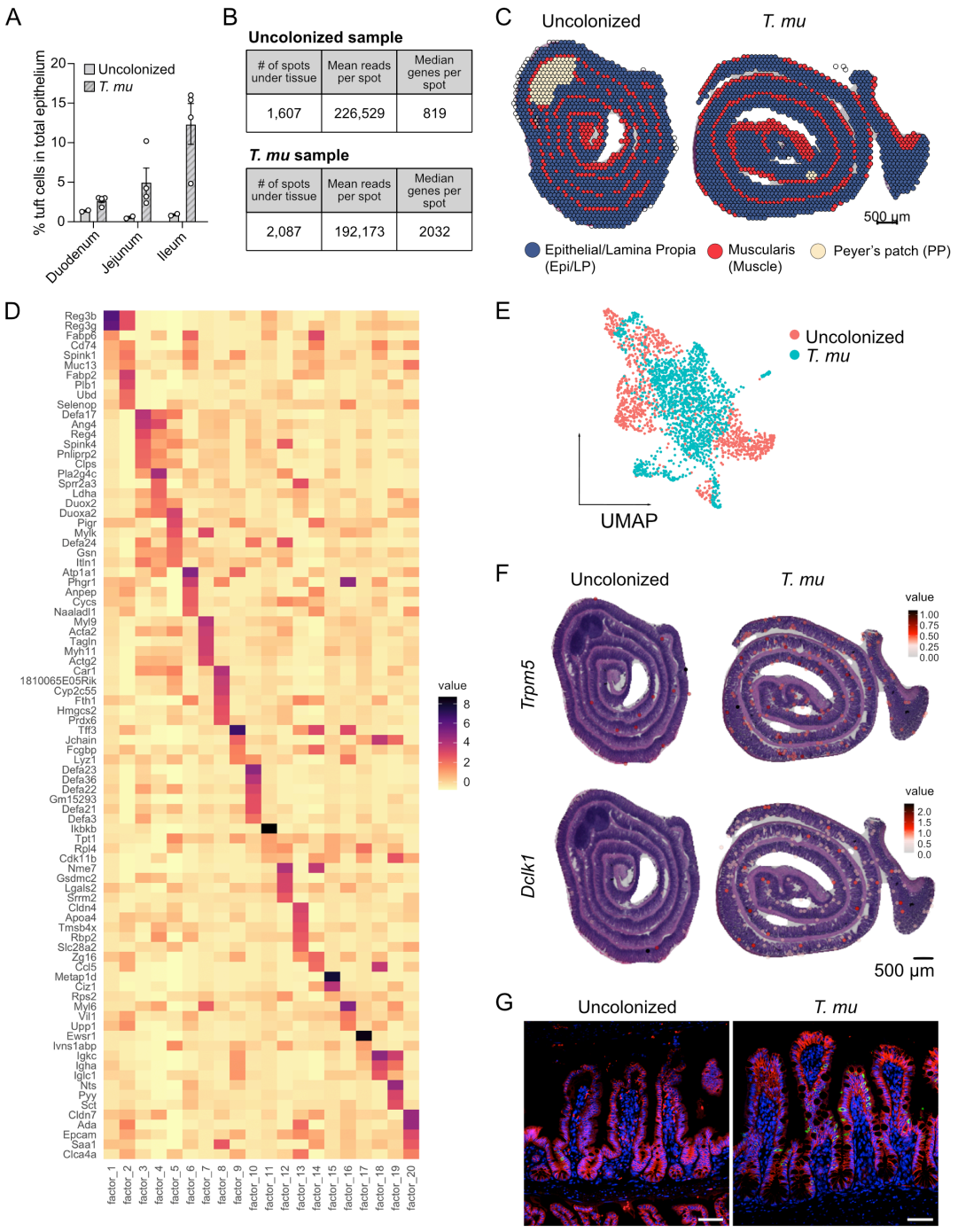

Fig. S1. *T. mu* colonization induces profound small intestinal epithelial remodeling.
(A) SI tuft cell frequency in uncolonized or *T. mu*-colonized *Gfi1b*$^{EGFP/+}$ mice, in which tuft cells are specifically marked with EGFP, determined by flow cytometry (n = 2 to 4 mice per group). Center values = arithmetic mean; errors bars = SEM.
(B) Summary of the number of spots sequenced, mean reads per spot, and the median genes per spot for both uncolonized and *T. mu*-colonized tissue sections that were used for spatial transcriptomics (ST) analysis.
(C) Manual annotations of tissue compartments (Epithelial/Lamina Propria, Muscularis, or Peyer's patch) overlaid onto the ST spots.
(D) Non-negative matrix factor analysis on the uncolonized and *T. mu*-colonized ST samples.

(E) Harmonized UMAP plot colored by sample identity to highlight the overlap of clusters shared between the treatment groups (uncolonized or *T. mu*-colonized).
(F) Gene features overlay plots on ST spots throughout ileal tissue of the uncolonized or *T. mu*-colonized mouse, depicting expression of canonical tuft cell-specific genes, *Trpm5* and *Dclk1*.
(G) Representative fluorescence microscopy images of the ileum from uncolonized or *T. mu*-colonized mice that were used for ST analysis. Nuclei (blue), E-cadherin (red), DCLK1 (green). Scale bar: 50 μm.

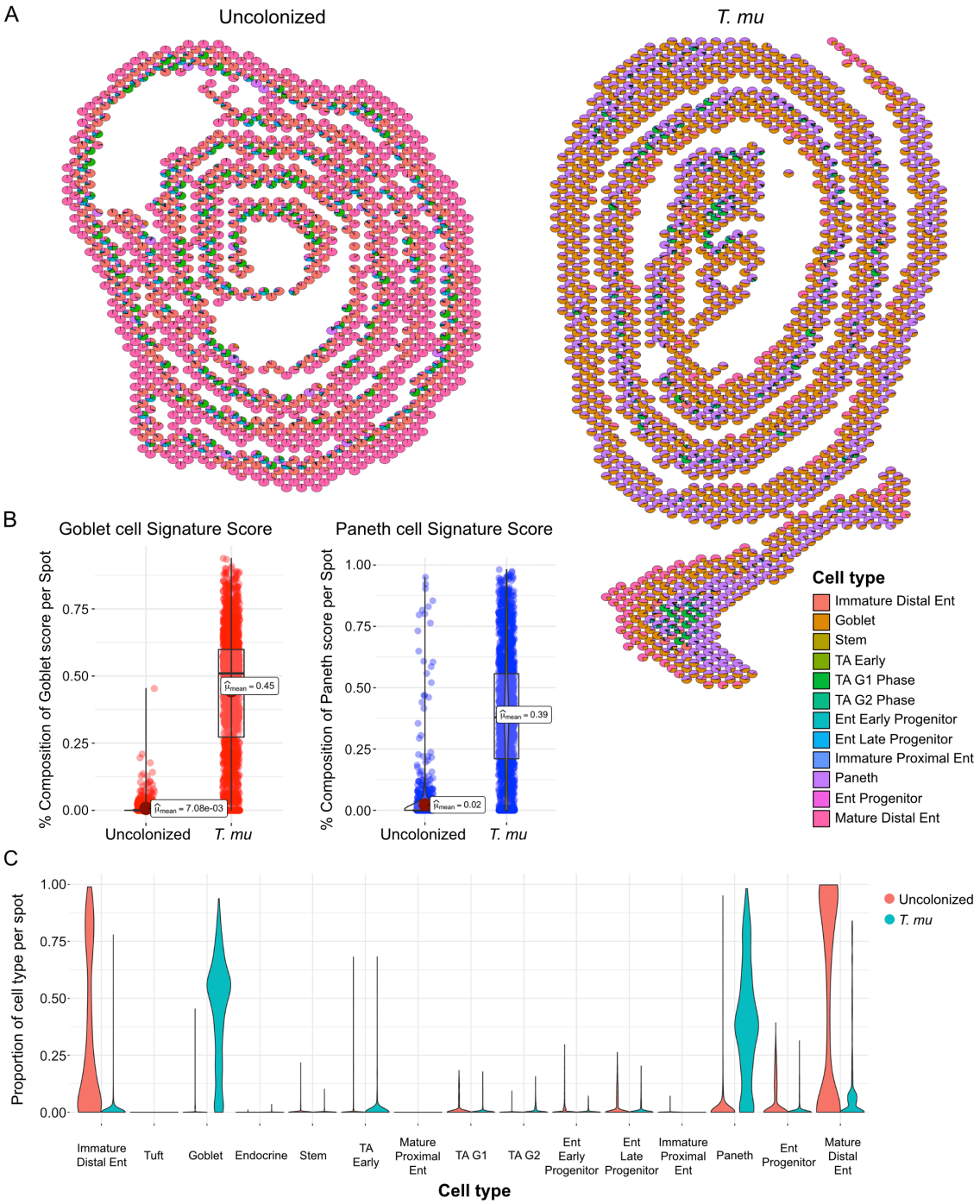

Fig. S2. Single-cell RNA sequencing (scRNA-seq) integration reveals epithelial cell identity in ST spots. (A) Scatter pie plots of uncolonized (left) and *T. mu*-colonized (right) samples, colored by annotated cell identities. Ent, Enterocyte; TA, Transit-amplifying; G1, G1/S cell-cycle phase; G2, G2/M cell-cycle phase. (B) Box plot of ST spots scored on the composition of goblet (left; red) or Paneth cell (right; blue) score in the uncolonized and *T. mu*-colonized mice.
(C) Violin plot of predicted epithelial cell types depicted for the two ST samples. Cell type identities were deconvoluted from scRNA-seq data from Haber et al., (2017) (9).

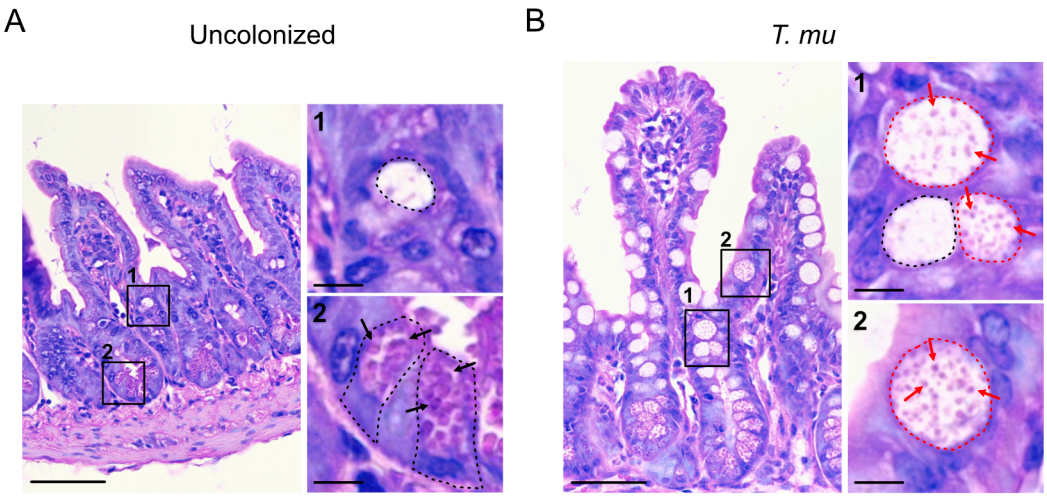

Fig. S3. *T. mu* colonization increases the abundance of "intermediate cells" with hybrid goblet and Paneth cell morphologies.
(A) Representative image of an H&E-stained section of several ileal crypt-villus axes from the uncolonized mouse used for ST analysis. Insets mark zoomed-in images to the right. 1: Dotted lines trace the outline of a goblet cell. 2: Dotted lines trace the outlines of individual Paneth cells. Arrows indicate representative Paneth cell secretory granules, which are round and stain light purple. Scale bar: 50 μm (original image), 10 μm (zoomed images).
(B) Representative image of an H&E-stained section of several ileal crypt-villus axes from the *T. mu*-colonized mouse used for ST analysis. Insets mark zoomed-in images to the right. 1 and 2: Black dotted lines trace the outline of a goblet cell. Red dotted lines trace the outlines of individual "intermediate cells" with hybrid goblet-Paneth morphologies; red arrows indicate representative granules, which stain light purple, within these cells. Scale bar: 50 μm (original image), 10 μm (zoomed images).

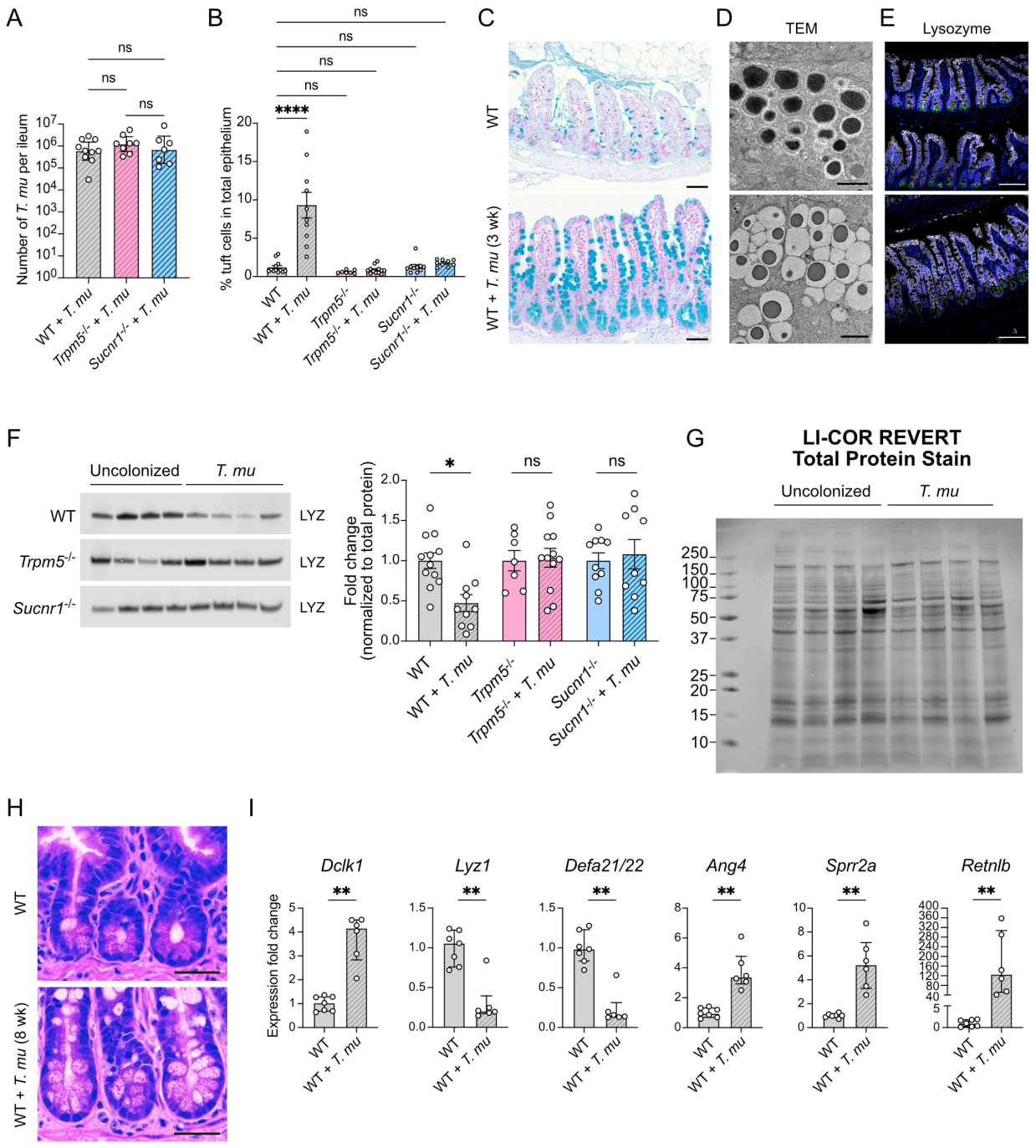

Fig. S4. *T. mu* alters Paneth cell biology and AMP production by stimulating tuft cell taste-chemosensory pathways.
(A) Quantitative PCR (qPCR) enumeration of *T. mu* abundance in the ilea of protist-colonized (3 wk) wild-type (WT), *Trpm5*$^{-/-}$, and *Sucnr1*$^{-/-}$ mice (n = 7 to 10 mice per group). Center values = geometric mean; error bars = 95% confidence interval (CI). Significance determined using a generalized linear model (GLM).
(B) Ileal tuft cell frequency in uncolonized or *T. mu*-colonized (3 wk) WT, *Trpm5*$^{-/-}$, and *Sucnr1*$^{-/-}$ mice as determined by flow cytometry (n = 7 to 10 mice per group). Center values = geometric mean; error bars = 95% CI. Significance determined using an ordinary one-way ANOVA test.

(C) Representative images of the ileum from uncolonized (top) or *T. mu*-colonized (3 wk) WT mice (bottom), stained with Alcian blue and nuclear fast red to identify goblet cells. Alcian blue dye stains acidic polysaccharides; nuclear fast red stains nuclei. Scale bar: 50 μm.
(D) Representative transmission electron microscopy images of secretory granules within Paneth cells in the ileal crypts from uncolonized or *T. mu*-colonized (3 wk) WT mice. Scale bar: 2 μm.
(E) Representative fluorescence microscopy images of uncolonized or *T. mu*-colonized (3 wk) WT mouse ilea. Nuclei (blue), E-cadherin (white), Lysozyme (green). Scale bar: 100 μm.
(F) Representative western blot images and quantitative analysis of intracellular lysozyme (LYZ) levels in the ilea of uncolonized or *T. mu*-colonized (3 wk) WT, *Trpm5*$^{-/-}$, and *Sucnr1*$^{-/-}$ mice. Each band and symbol represents an individual mouse. LYZ levels were normalized to REVERT total protein stain (refer to Fig. S4G for an example image of REVERT staining corresponding to the blots) (n = 7 to 12 mice per group). Center values = arithmetic mean; error bars = SEM. A linear mixed model was used to determine significance.
(G) Representative Western blot membrane of WT uncolonized or *T. mu*-colonized samples from Fig. S4F stained with REVERT total protein stain. REVERT total protein stain was used for normalization to determine relative intracellular LYZ levels in the different experimental samples.
(H) Representative images of H&E-stained sections of the ileal crypts from uncolonized or *T. mu*-colonized (8 wk) WT mice. Scale bar: 25 μm.
(I) Expression of *Dclk1* (tuft cell marker) and representative AMP genes determined by qRT-PCR in the ileal epithelial fraction from uncolonized or *T. mu*-colonized (8 wk) WT mice (n = 6 to 7 mice per group). Relative expression normalized to *Gapdh*. Center values = median; error bars = interquartile range (IQR). Significance determined using Mann-Whitney *U* test.
ns = no significance, * $p < 0.05$, ** $p < 0.01$, **** $p < 0.0001$.

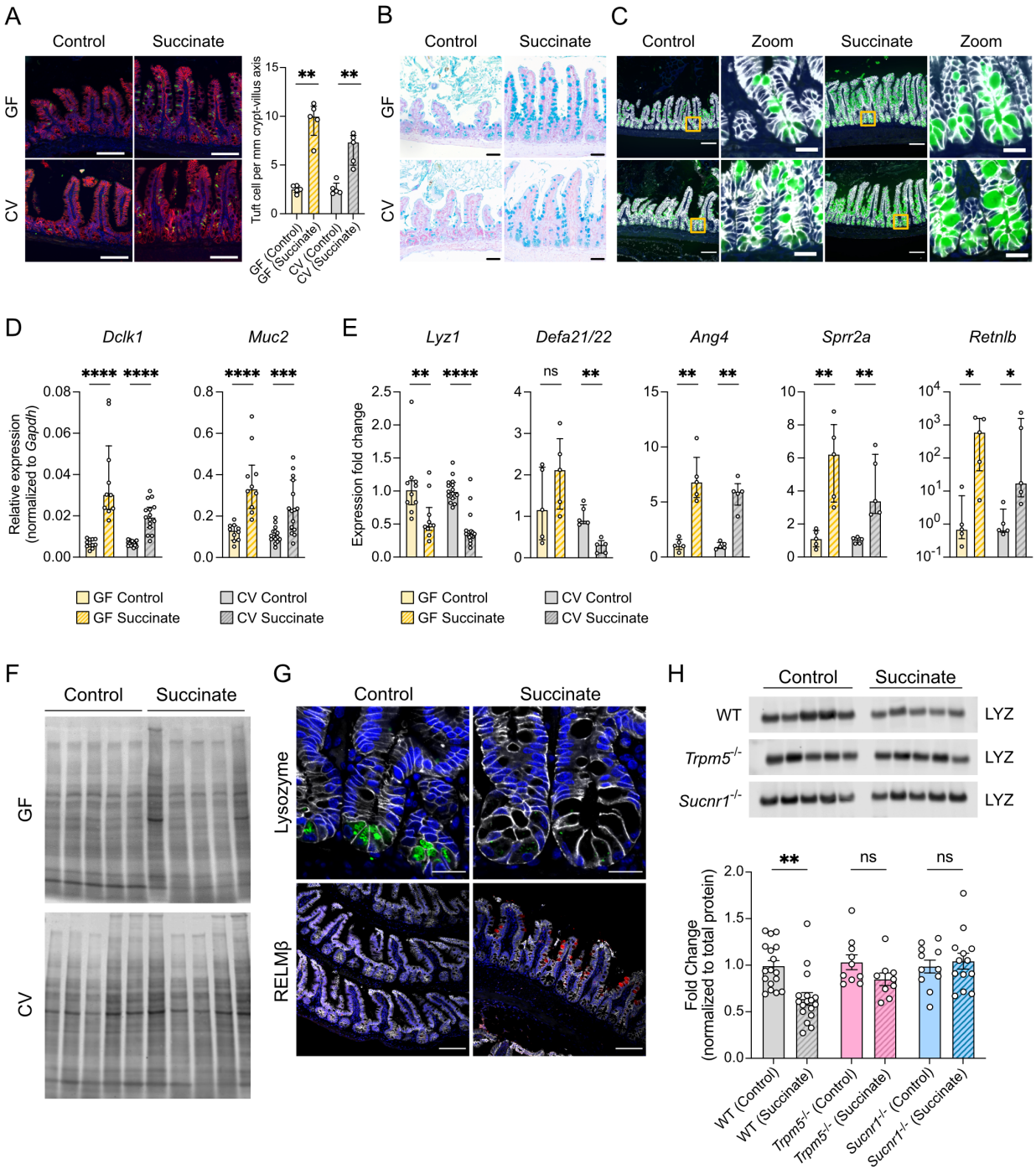

Fig. S5. Succinate treatment led to tuft cell expansion and AMP changes in WT mice, but not in mice lacking tuft cell chemosensory components required to detect this metabolite.
(A) The number of tuft cells per mm of crypt-villus axis were quantified for control or succinate-treated (1 wk) germ-free (GF) or conventionally colonized (CV) WT mice (n = 5 mice per group). Center values = median; error bars = IQR. Significance determined using Mann-Whitney *U* test. Representative fluorescence microscopy images of each experimental condition are shown on the left. Nuclei (blue), E-cadherin (red), DCLK1 (green). Scale bar: 100 μm.
(B) Representative images of the ileum from control or succinate-treated (1 wk) GF or CV mice, stained with Alcian blue and nuclear fast red to identify goblet cells. Scale bar: 50 μm.

(C) Representative fluorescence microscopy images of the ileum from control or succinate-treated (1 wk) GF or CV WT mice. Nuclei (blue), E-cadherin (white), MUC2 (green). Insets mark zoomed images (right). Scale bar: 100 μm (original image), 20 μm (zoomed images).
(D) Expression of *Dclk1* (tuft cell marker) and *Muc2* (goblet cell marker) determined by qRT-PCR in the ilea of control or succinate-treated (1 wk) GF and CV mice (n = 10 to 15 mice per group). Relative expression normalized to *Gadph*. Center values = median; error bars = IQR. Significance determined using Mann-Whitney *U* test.
(E) Expression of representative AMP genes determined by qRT-PCR in the ilea of control or succinate-treated GF and CV mice (n = 5 to 15 mice per group). Relative expression normalized to *Gapdh*. These are the same samples as in Fig. 4C, but expression is shown as expression fold change (where the control mean is set to 1). Center values = median; error bars = IQR. Significance determined using Mann-Whitney *U* test.
(F) Representative western blot membranes of control or succinate-treated GF or CV WT mice (shown in Fig. 4D) stained with REVERT total protein stain. REVERT total protein stain was used for normalization to determine relative intracellular lysozyme levels in the different experimental samples. Images were cropped to remove samples that were unrelated to the experiment.
(G) Representative fluorescence microscopy images of the ileum from control or succinate-treated (1 wk) CV WT mice. Nuclei (blue), E-cadherin (white), Lysozyme (green), RELMβ (red). Scale bar: 20 μm (top images), 100 μm (bottom images).
(H) Representative western blot images and quantitative analysis of intracellular lysozyme (LYZ) levels in the ilea of control or succinate-treated (1 wk) WT, *Trpm5*$^{-/-}$, and *Sucnr1*$^{-/-}$ mice. Each band and symbol represents an individual mouse. LYZ levels were normalized to REVERT total protein stain (n = 9 to 17 mice per group). Center values = arithmetic mean; error bars = SEM. A linear mixed model was used to determine significance.
ns = no significance, * $p < 0.05$, ** $p < 0.01$, *** $p < 0.001$, **** $p < 0.0001$.

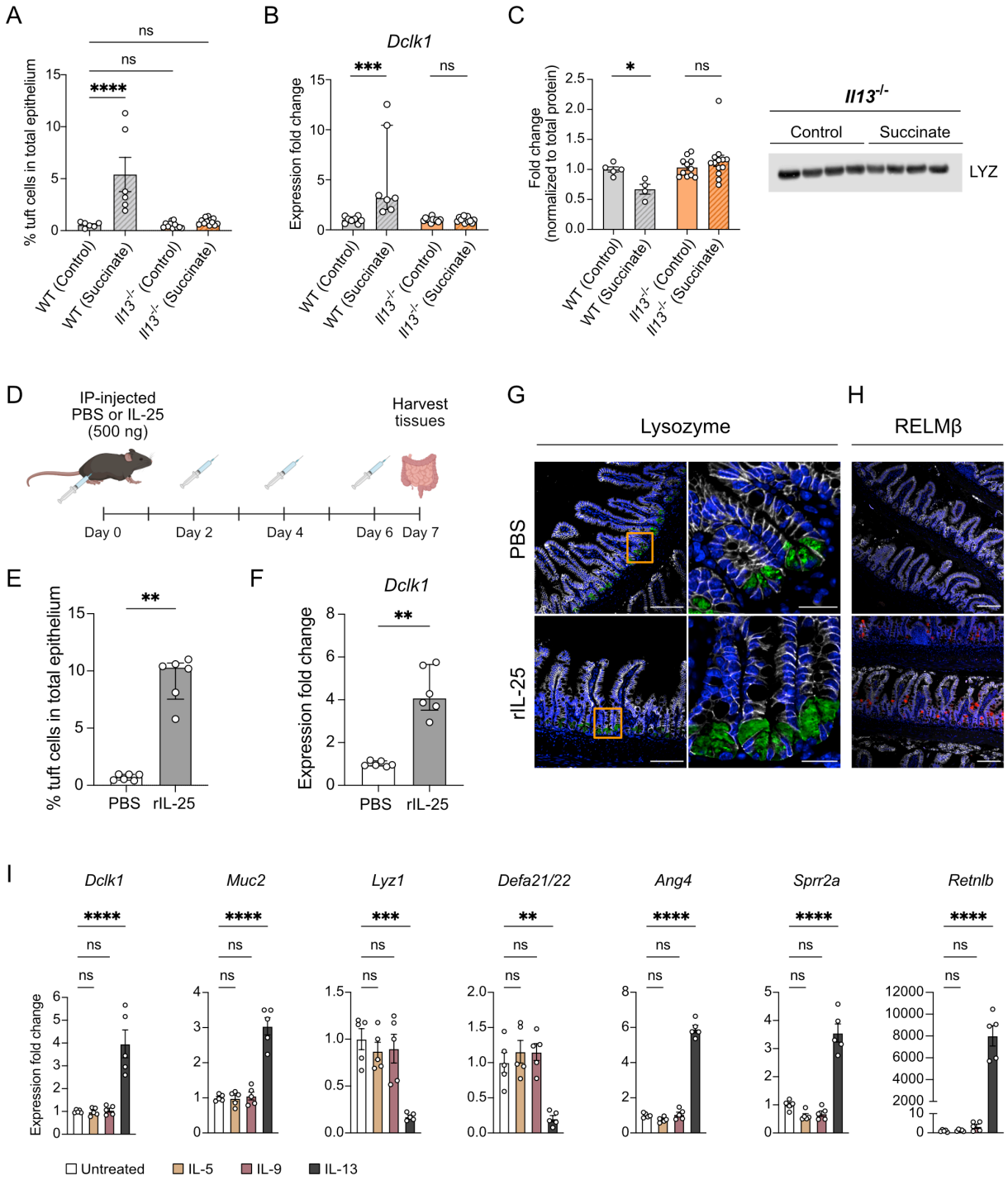

Fig. S6. Type 2 immunity is required for changes to antimicrobial production downstream of tuft cell stimulation.
(A) Ileal tuft cell frequency in control or succinate-treated (1 wk) WT or *Il13*$^{-/-}$ mice determined by flow cytometry (n = 6 to 12 mice per group). Center values = arithmetic mean; error bars = SEM. Significance determined using ordinary one-way ANOVA test.

(B) Expression of *Dclk1* determined by qRT-PCR in the ileal epithelial fraction of control or succinate-treated (1 wk) WT and *Il13*$^{-/-}$ mice (n = 7 to 13 mice per group).
(C) Representative western blot images and quantitative analysis of intracellular lysozyme (LYZ) levels in the ilea of control or succinate-treated (1 wk) WT and *Il13*$^{-/-}$ mice. Each band and symbol represents an individual mouse. LYZ levels were normalized to REVERT total protein stain (n = 4 to 14 mice per group). Center values = arithmetic mean; error bars = SEM. A linear mixed model was used to determine significance.
(D) Schematic of recombinant IL-25 injections. PBS (vehicle control) or 500 ng IL-25 were intraperitoneally (IP)-injected into mice every other day for 1 wk, after which ileal tissues were harvested for downstream analyses.
(E) Ileal tuft cell frequency in WT mice IP-injected with PBS or IL-25 determined by flow cytometry (n = 6 mice per group). Center values = median; error bars = IQR. Significance determined using Mann-Whitney *U* test.
(F) Expression of *Dclk1* determined by qRT-PCR in the ileal epithelial fraction of WT mice IP-injected with PBS or IL-25 (n = 6 mice per group). Center values = median; error bars = IQR. Significance determined using Mann-Whitney *U* test.
(G and H) Representative fluorescence microscopy images of the ileum from PBS or IL-25 injected WT mice. (G) Nuclei (blue), E-cadherin (white), Lysozyme (green). The insets mark zoomed in regions (right images). Scale bar: 100 μm (left images), 20 μm (right images). (H) Nuclei (blue), E-cadherin (white), RELMβ (red). Scale bar: 100 μm.
(I) Expression of *Dclk1* (tuft cell marker), *Muc2* (goblet cell marker), and representative AMP genes determined by qRT-PCR in untreated, IL-5, IL-9, or IL-13 treated ileal organoids (n = 5 samples per group). Center values = arithmetic mean; error bars = SEM. Significance determined using ordinary one-way ANOVA test.
For qRT-PCR data, relative expression normalized to *Gapdh*. ns = no significance, * $p < 0.05$, ** $p < 0.01$, *** $p < 0.001$, **** $p < 0.0001$.

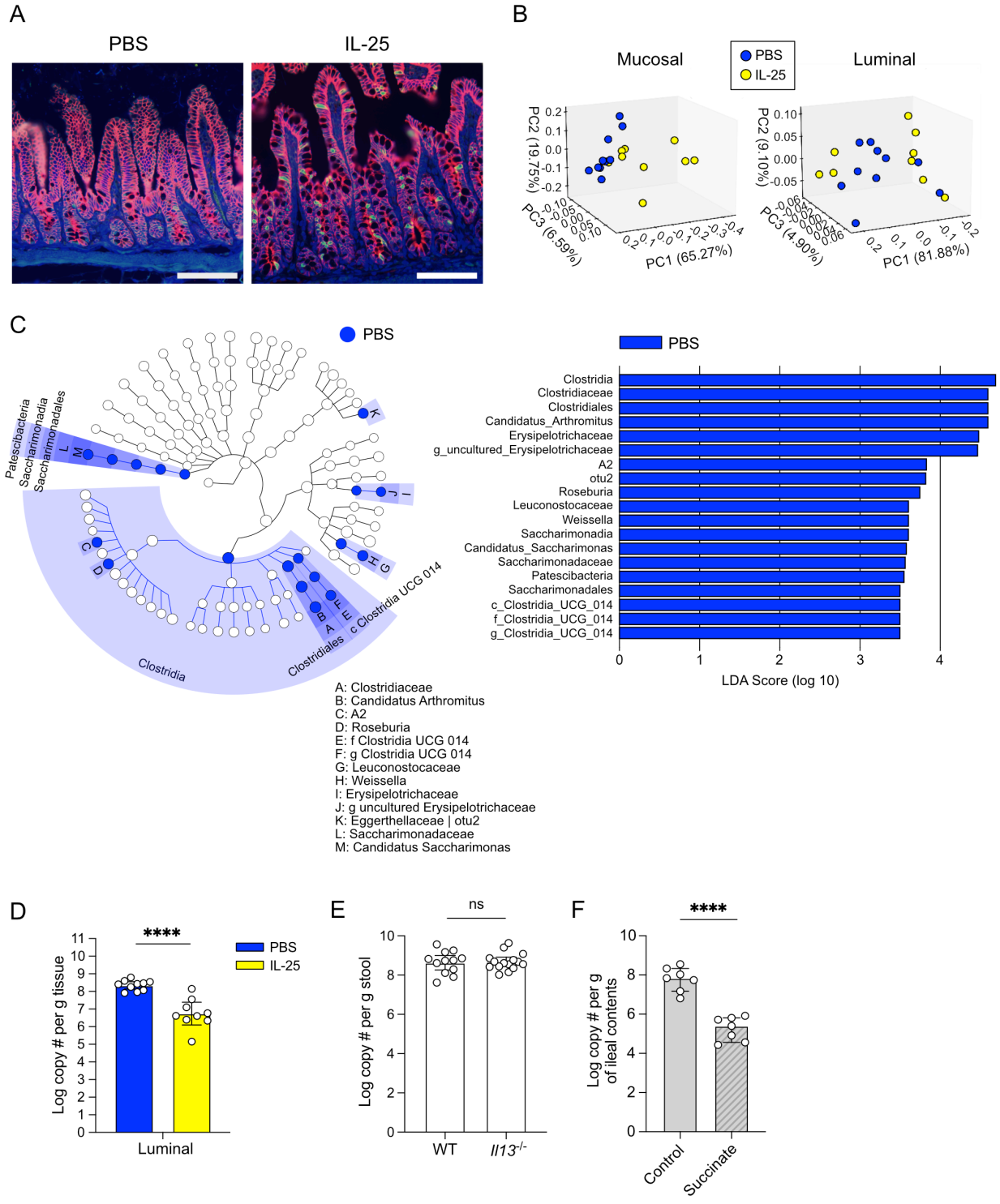

Fig. S7. Recombinant IL-25 injections induce type 2 immunity and alter the ileal microbiome.
(A) Representative fluorescence microscopy images of the ileum of PBS or IL-25 injected WT Taconic mice used for 16S rRNA gene sequencing experiment. Nuclei (blue), E-cadherin (red), DCLK1 (green). Scale bar: 100 μm.
(B) Weighted UniFrac PCoA plots depicting differences in microbial communities in mucosal or luminal samples. The 1st, 2nd, and 3rd principal components indicate the percentage of variation explained by the

principal components for the ileal mucosal or luminal communities of PBS or IL-25 injected mice. Mucosal, $p = 0.007$; Luminal, $p = 0.077$. Significance determined via PERMANOVA test.
(C) Linear discriminant analysis (LDA) Effect Size (LEfSe) analysis using a LDA threshold score of 2 to identify ileal luminal bacterial taxa in PBS or IL-25 injected mice (n = 9 to 10 mice per group). Only PBS-injected mice showed differentially enriched taxa. Cladogram (left) highlights taxonomic relatedness of bacteria while LDA plot (right) is an ordered list of enriched bacteria.
(D) Absolute quantification of SFB 16S rRNA gene copies in the ileal luminal fraction of PBS or IL-25 injected mice (n = 9 to 10 mice per group).
(E) Absolute quantification of SFB 16S rRNA gene copies in the stool of WT (Taconic) and *Il13*$^{-/-}$ mice after 2 wk of co-housing (n = 12 to 15 mice per group). This is to confirm that *Il13*$^{-/-}$ mice have acquired SFB prior to IL-25 injections as shown in Fig. 6E.
(F) Absolute quantification of SFB 16S rRNA gene copies in the small intestinal contents of control or succinate-treated (2 wk) WT mice (n = 7 mice per group).
In Panels D-F, center values = geometric mean; error bars = 95% CI. Significance determined using a generalized linear model. ns = no significance, **** $p < 0.0001$.

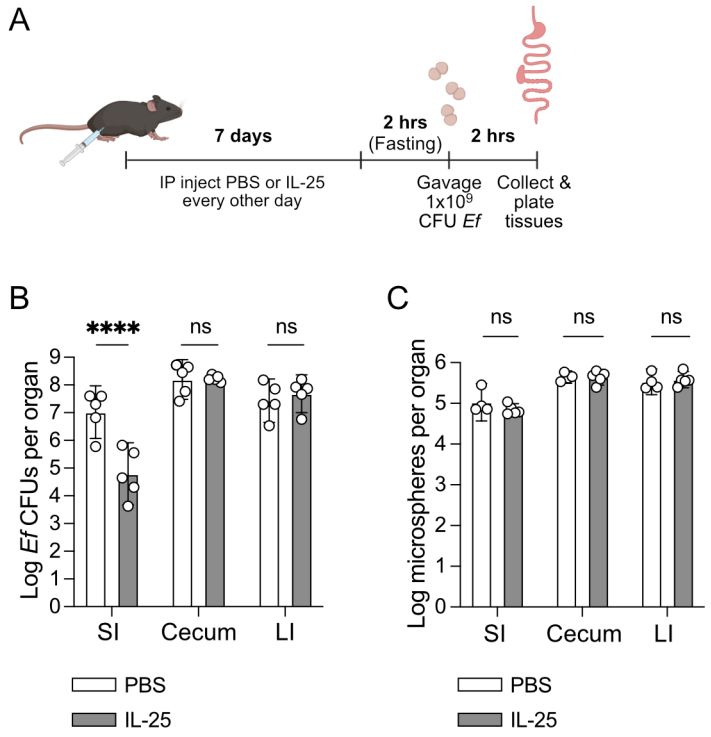

Fig. S8. Type 2 immune induction decreases the abundance of the gut commensal *Enterococcus faecalis* in the small intestine.
(A) Experimental schematic. WT mice were IP-injected with PBS or IL-25 as described in Fig. S6D, and then orally inoculated with *Enterococcus faecalis* (*Ef*).
(B) *Ef* CFUs per organ were enumerated in the small intestine (SI), cecum, and large intestine (LI) (n = 5 mice per group).
(C) WT mice were IP-injected with PBS or IL-25 as described in Fig. S8A, and then orally-inoculated with fluorescent microspheres (instead of *Ef*) to assess differences in gut motility between both experimental conditions. The luminal contents of the small intestine (SI), cecum, and large intestine (LI) were collected from each mouse at 2 hrs post-gavage for quantification of total microspheres per organ (n = 5 mice per group).
In Panels B and C, center values = geometric mean; error bars = 95% CI. Significance determined using a generalized linear model. ns = no significance, **** $p < 0.0001$.

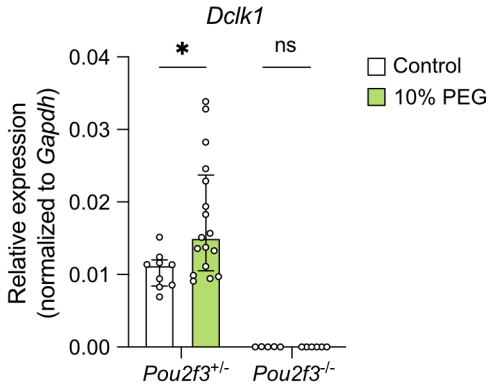

Fig. S9. Polyethylene glycol (PEG) treatment induces tuft cell hyperplasia.
Expression of tuft cell marker *Dclk1* determined by qRT-PCR in the ileal epithelial fraction of untreated or PEG-treated *Pou2f3*$^{+/-}$ or *Pou2f3*$^{-/-}$ littermates (n = 5 to 17 mice per group). No *Dclk1* expression was detected in the ileal epithelia of *Pou2f3*$^{-/-}$ mice, confirming that these animals lack tuft cells. Relative expression normalized to *Gapdh*. Center values = median; error bars = IQR. Significance determined using Mann-Whitney *U* test. ns = no significance, * $p < 0.05$.

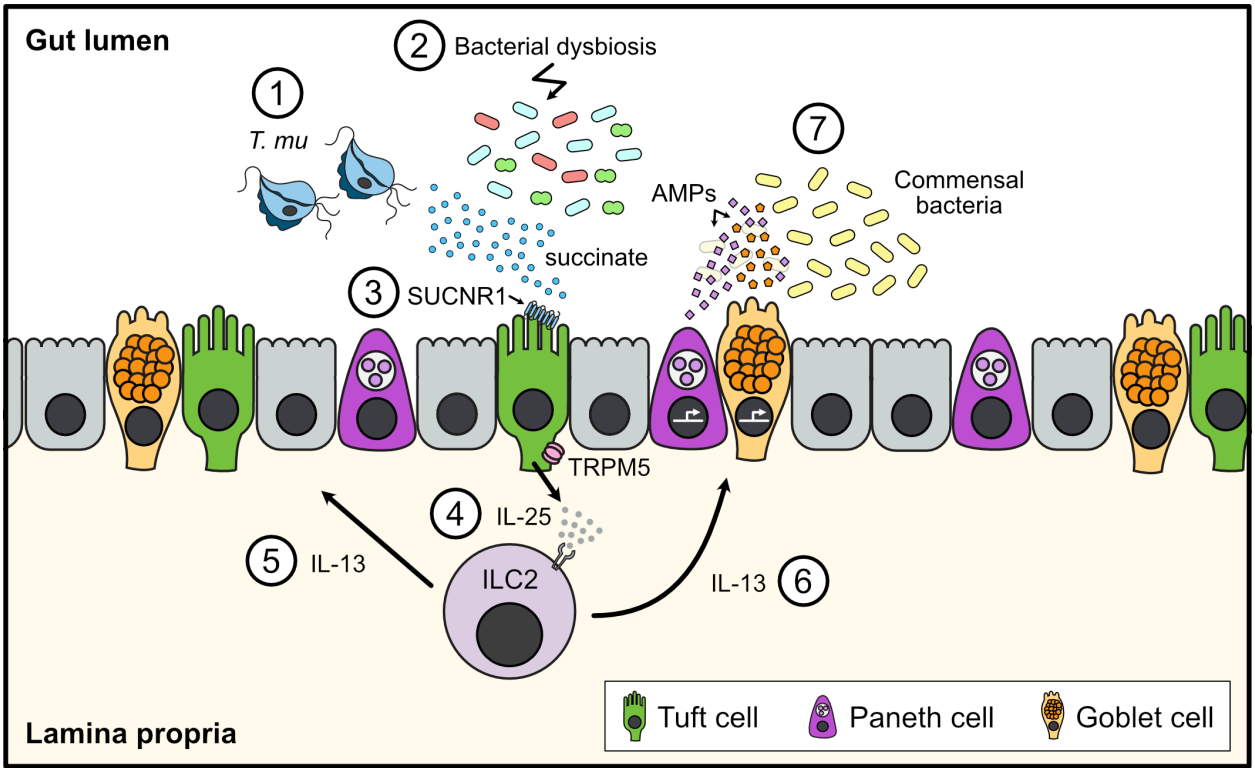

Fig. S10. Model of how microbial-derived succinate remodels the small intestinal epithelial and antimicrobial landscape.
Colonization with the commensal protist *T. mu* (1) or bacterial dysbiosis (2) leads to a spike in luminal succinate levels in the distal small intestine, which engages the succinate receptor SUCNR1 on tuft cells (3). This activates taste-chemosensory transduction in tuft cells, culminating in the opening of the ion channel TRPM5 and release of IL-25 from tuft cells, which activate group 2 innate lymphoid cells (ILC2s) (4). ILC2s produce IL-13, which stimulates intestinal stem cells to differentiate into tuft, goblet, and Paneth cells, leading to hyperplasia of all three cell types (5). IL-13 also alters AMP expression in goblet and Paneth cells (6), although it is unclear if the cytokine acts directly on these cell types or alters AMP expression at the cellular differentiation stage. These shifts in AMP production lead to increased killing of specific commensal bacterial species (7). Tuft cells may have evolved to sense increased bacterial succinate levels secondary to dysbiosis and alter AMP expression in response to restore community homeostasis. *T. mu* may have incidentally engaged this pathway given that they produce copious amounts of succinate as a metabolic byproduct.

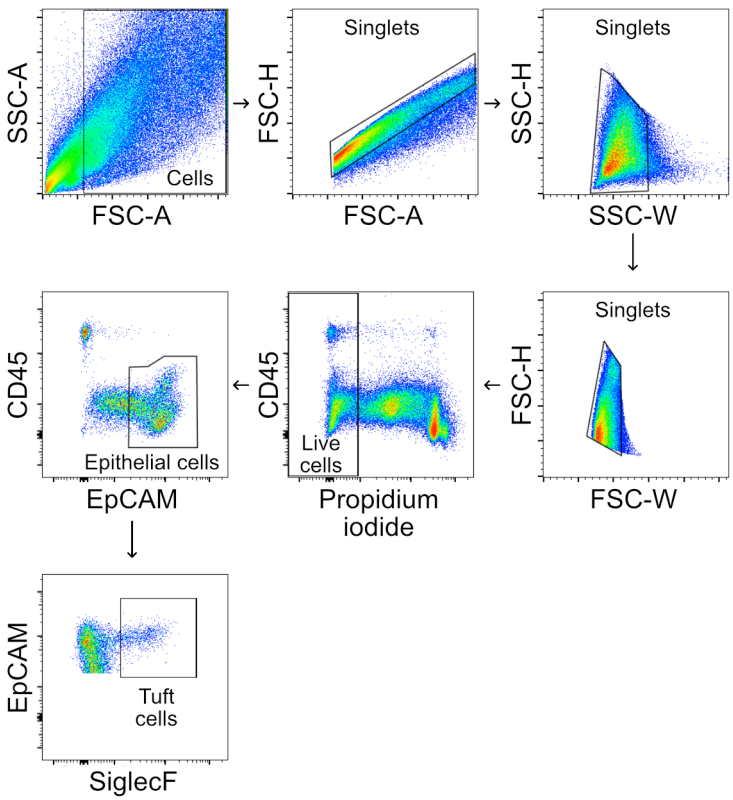

Fig. S11. Tuft cell gating strategy for flow cytometry.
Epithelial cells from the distal small intestine were isolated and gated on viable $CD45^{-}$ $EpCAM^{+}$ cells. Tuft cells were further selected as $SiglecF^{+}$.

Table S1. Primer sequences.

Primer	Sequence (5' – 3')	Source
qRT-PCR Primers		
Gapdh for	CCTCGTCCCGTAGACAAAATG	(11)
Gapdh rev	TCTCCACTTTGCCACTGCAA	(11)
Dclk1 for	CAGCCTGGACGAGCTGGTGG	(10)
Dclk1 rev	TGACCAGTTGGGGTTCACAT	(10)
Muc2 for	CCATTGAGTTTGGGAACATGC	(11)
Muc2 rev	TTCGGCTCGGTGTTCAGAG	(11)
Klf4 for	ATCCTTTCCAACTCGCTAACCC	(11)
Klf4 rev	CGGATCGGATAGCTGAAGCTG	(11)
Lyz1 for	GCCAAGGTCTACAATCGTTGTGAGTTG	(31)
Lyz1 rev	CAGTCAGCCAGCTTGACACCACG	(31)
Defa21/22 for	CCAGGGGAAGATGACCAGGCTG	(31)
Defa21/22 rev	TGCAGCGACGATTTCTACAAAGGC	(31)
Sprr2a for	CCTTGTCCTCCCCAAGTG	(2)
Sprr2a rev	AGGGCATGTTGACTGCCAT	(2)
Retnlb for	GCTCTTCCCTTTCCTTCTCCAA	(32)
Retnlb rev	AACACAGTGTAGGCTTCATGCTGTA	(32)
Ang4 for	TTGGCTTGGCATCATAGT	(33)
Ang4 rev	CCAGCTTTGGAATCACTG	(33)
Il25 for	ACAGGGACTTGAATCGGGTC	(10)
Il25 rev	TGGTAAAGTGGGACGGAGTTG	(10)
qPCR Primers		
T. musculis 28S rRNA for	GCTTTTGCAAGCTAGGTCCC	(10)
T. musculis 28S rRNA rev	TTTCTGATGGGGCGTACCAC	(10)
UniF340	ACTCCTACGGGAGGCAGCAGT	(14)
UniR514	ATTACCGCGGCTGCTGGC	(14)
SFB736F	GACGCTGAGGCATGAGAGCAT	(14)
SFB844R	GACGGCACGGATTGTTATTCA	(14)

Table S2. Antibodies and flow reagents.

Antibodies	Clone	Source	RRID
Flow cytometry			
Anti-CD16/CD32	93	BioLegend	AB_312801
Anti-CD45	30-F11	BioLegend	AB_493535
Anti-CD326 (EpCAM)	G8.8	BioLegend	AB_1236471 (PE/Cy7); AB_1134102 (APC)
Anti-Siglec-F	E50-2440	BD Biosciences	AB_2687570
Microscopy			
Anti-DCLK1	Polyclonal	Abcam	AB_873538
Anti-E-Cadherin	36	BD Biosciences	AB_397580
Anti-Lysozyme	Polyclonal	Agilent	AB_2341231
Anti-RELM*β*	Polyclonal	PeproTech	AB_1268845
Anti-MUC2	EPR23479-47	Abcam	AB_2888616
Western blot			
Anti-Lysozyme	EPR2994(2)	Abcam	AB_10861277
IRDye® 800CW Goat anti-rabbit IgG (H+L)	--	LI-COR Biosciences	AB_621843
IRDye® 800CW Donkey anti-rabbit IgG (H+L)	--	LI-COR Biosciences	AB_2715510

References

1. L. V. Hooper, T. S. Stappenbeck, C. V. Hong, J. I. Gordon, Angiogenins: a new class of microbicidal proteins involved in innate immunity. *Nat Immunol* **4**, 269–273 (2003).

2. Z. Hu, *et al.*, Small proline-rich protein 2A is a gut bactericidal protein deployed during helminth infection. *Science* **374**, eabe6723 (2021).

3. D. Sorobetea, M. Svensson-Frej, R. Grencis, Immunity to gastrointestinal nematode infections. *Mucosal Immunol* **11**, 304–315 (2018).

4. S. Damak, *et al.*, Trpm5 Null Mice Respond to Bitter, Sweet, and Umami Compounds. *Chemical Senses* **31**, 253–264 (2006).

5. K. J. Stanya, *et al.*, Direct control of hepatic glucose production by interleukin-13 in mice. *J Clin Invest* **123**, 261–271 (2013).

6. F. C. Walker, *et al.*, Norovirus evolution in immunodeficient mice reveals potentiated pathogenicity via a single nucleotide change in the viral capsid. *PLOS Pathogens* **17**, e1009402 (2021).

7. I. I. Ivanov, *et al.*, Induction of Intestinal Th17 Cells by Segmented Filamentous Bacteria. *Cell* **139**, 485–498 (2009).

8. J. Bergenstråhle, L. Larsson, J. Lundeberg, Seamless integration of image and molecular analysis for spatial transcriptomics workflows. *BMC Genomics* **21**, 1–7 (2020).

9. A. L. Haber, *et al.*, A single-cell survey of the small intestinal epithelium. *Nature* **551**, 333–339 (2017).

10. M. R. Howitt, *et al.*, Tuft cells, taste-chemosensory cells, orchestrate parasite type 2 immunity in the gut. *Science* **351**, 1329–1333 (2016).

11. M. R. Howitt, *et al.*, The Taste Receptor TAS1R3 Regulates Small Intestinal Tuft Cell Homeostasis. *ImmunoHorizons* **4**, 23–32 (2020).

12. H. Miyoshi, T. S. Stappenbeck, *In vitro* expansion and genetic modification of gastrointestinal stem cells in spheroid culture. *Nature Protocols* **8**, 2471–2482 (2013).

13. T. Sato, H. Clevers, “Primary Mouse Small Intestinal Epithelial Cell Cultures” in *Epithelial Cell Culture Protocols: Second Edition*, Methods in Molecular Biology., S. H. Randell, M. L. Fulcher, Eds. (Humana Press, 2013), pp. 319–328.

14. M. Barman, *et al.*, Enteric Salmonellosis Disrupts the Microbial Ecology of the Murine Gastrointestinal Tract. *Infection and Immunity* **76**, 907–915 (2008).

15. E. Bolyen, *et al.*, Reproducible, interactive, scalable and extensible microbiome data science using QIIME 2. *Nat Biotechnol* **37**, 852–857 (2019).

16. M. Martin, Cutadapt removes adapter sequences from high-throughput sequencing reads. *EMBnet.journal* **17**, 10–12 (2011).

17. B. J. Callahan, *et al.*, DADA2: High-resolution sample inference from Illumina amplicon data. *Nat Methods* **13**, 581–583 (2016).

18. K. Katoh, D. M. Standley, MAFFT Multiple Sequence Alignment Software Version 7: Improvements in Performance and Usability. *Mol Biol Evol* **30**, 772–780 (2013).

19. D.J. Lane, "16S/23S rRNA sequencing" in Nucleic Acid Techniques in Bacterial Systematics, E. Stackebrandt, M. Goodfellow, Eds. (John Wiley and Sons, 1991), pp. 115-175.

20. M. N. Price, P. S. Dehal, A. P. Arkin, FastTree 2 – Approximately Maximum-Likelihood Trees for Large Alignments. *PLOS ONE* **5**, e9490 (2010).

21. T. Z. DeSantis, *et al.*, Greengenes, a Chimera-Checked 16S rRNA Gene Database and Workbench Compatible with ARB. *Applied and Environmental Microbiology* **72**, 5069–5072 (2006).

22. M. J. Anderson, A new method for non-parametric multivariate analysis of variance. *Austral Ecology* **26**, 32–46 (2001).

23. J. G. Caporaso, *et al.*, QIIME allows analysis of high-throughput community sequencing data. *Nat Methods* **7**, 335–336 (2010).

24. W. H. Kruskal, W. A. Wallis, Use of Ranks in One-Criterion Variance Analysis. *Journal of the American Statistical Association* **47**, 583–621 (1952).

25. Y. Vázquez-Baeza, M. Pirrung, A. Gonzalez, R. Knight, EMPeror: a tool for visualizing high-throughput microbial community data. *Gigascience* **2**, 16 (2013).

26. Y. Vázquez-Baeza, *et al.*, Bringing the Dynamic Microbiome to Life with Animations. *Cell Host & Microbe* **21**, 7–10 (2017).

27. G. Van Rossum, F. L. Drake, *Python 3 Reference Manual* (CreateSpace, 2009).

28. N. Segata, *et al.*, Metagenomic biomarker discovery and explanation. *Genome Biol* **12**, 1–18 (2011).

29. F. Asnicar, G. Weingart, T. L. Tickle, C. Huttenhower, N. Segata, Compact graphical representation of phylogenetic data and metadata with GraPhlAn. *PeerJ* **3**, e1029 (2015).

30. G. M. Dunny, B. L. Brown, D. B. Clewell, Induced cell aggregation and mating in Streptococcus faecalis: evidence for a bacterial sex pheromone. *Proc Natl Acad Sci U S A* **75**, 3479–3483 (1978).

31. N. H. Salzman, *et al.*, Enteric defensins are essential regulators of intestinal microbial ecology. *Nature Immunology* **11**, 76–82 (2010).

32. W. He, *et al.*, Bacterial colonization leads to the colonic secretion of RELMβ/FIZZ2, a novel goblet cell-specific protein. *Gastroenterology* **125**, 1388–1397 (2003).

33. N. Burger-van Paassen, *et al.*, Mucin Muc2 Deficiency and Weaning Influences the Expression of the Innate Defense Genes Reg3β, Reg3γ and Angiogenin-4. *PLOS ONE* **7**, e38798 (2012).